

## Pyrimidine-based inhibitors of CaMKII $\delta$

Babu Mavunkel, Yong-jin Xu, Bindu Goyal, Don Lim, Qing Lu, Zheng Chen, Dan-Xiong Wang, Jeffrey Higaki, Indrani Chakraborty, Albert Liclican, Steve Sideris, Maureen Laney, Ulrike Delling, Rosanne Catalano, Linda S. Higgins, Hui Wang, Jing Wang, Ying Feng, Sundee Dugar and Daniel E. Levy\*

*Scios, Inc., 6500 Paseo Padre Parkway, Fremont, CA 94555, USA*

Received 6 December 2007; revised 21 February 2008; accepted 22 February 2008  
Available online 4 March 2008

**Abstract**—Non-ATP competitive pyrimidine-based inhibitors of CaMKII $\delta$  were identified. Computational studies were enlisted to predict the probable mode of binding. The results of the computational studies led to the design of ATP competitive inhibitors with optimized hinge interactions. Inhibitors of this class possessed improved enzyme and cellular activity compared to early leads.  
© 2008 Elsevier Ltd. All rights reserved.

The importance of calcium signaling to the regulation of biological pathways, along with the associated roles of the Ca<sup>2+</sup>/calmodulin-dependant kinases (CaMKs), was summarized in previous reports from our group.<sup>1–3</sup> In these reports, maleimide-based compounds capable of inhibiting a recombinant preparation of CaMKII $\delta$  were described. Concurrent to these studies, a class of pyrimidine-based CaMKII $\delta$  inhibitors was identified. The preparation of the initial lead series, shown in [Scheme 1](#), began with a Suzuki coupling<sup>4</sup> with 2,4-dichloropyrimidine generating compounds **3**. Buchwald coupling<sup>5</sup> of  $\alpha$ -S-methylbenzylamine with 2-chloro-4-nitropyridine followed by the reduction of the nitro group gave compound **6**. Compounds **3** and **6** were joined using Buchwald conditions.

As shown in [Table 1](#), the initial SAR studies resulted in a series of inhibitors with IC<sub>50</sub> values ranging from 1 to 3  $\mu$ M ([Table 1](#)) against the cloned enzyme.<sup>6</sup> These compounds were determined to be non-competitive inhibitors with respect to ATP. Furthermore, using a computationally generated homology model for CaMKII $\delta$ ,<sup>7</sup> these compounds were predicted to bind in a groove near the opening to the ATP site and pointing towards the solvent front. With this binding hypothesis in mind, one additional compound, **7f**, was prepared in order to provide better interactions with the solvent front residues. As the breakthrough structure, this com-

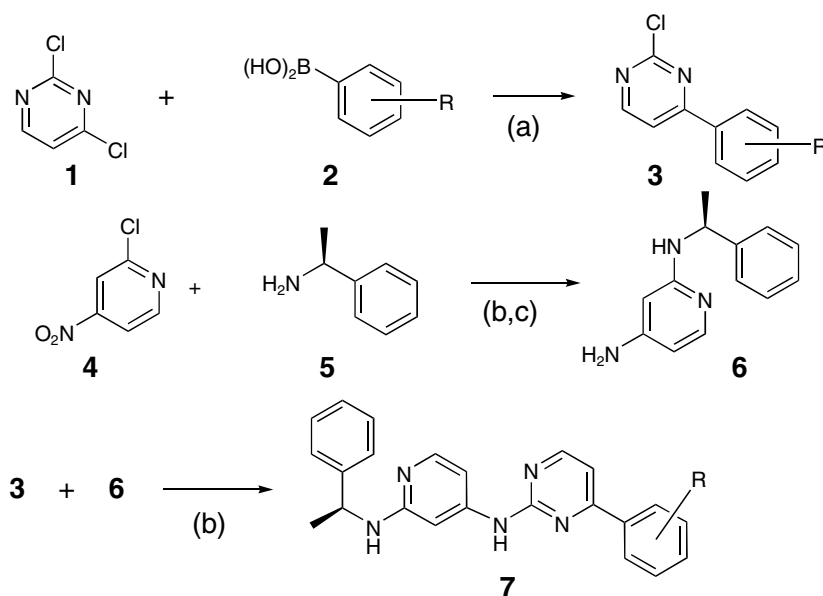
pound, for the first time, demonstrated sub-micromolar potency and was determined to bind competitively with ATP. This indicated that we were, at that time, interacting with the ATP site, itself. This hypothesis was further supported through computational analyses where the carboxylic acid of compound **7f** was shown capable of binding, via salt bridge, to Lys22 thus blocking the entrance to the ATP site.

Building upon the initial SAR, we studied the parameters surrounding the activity of **7f**. In particular, could the carboxylic acid be modified to alternate functionalities, isosteres or homologated analogs? To support this SAR, compounds **7g–i** were prepared according to [Scheme 1](#). Furthermore, compounds **7j** and **7l** were prepared from the methyl ester (**7e**) using standard conditions. Finally, the tetrazole analog **7k** was prepared from a nitrile generated according to [Scheme 1](#) and reacting the nitrile with TMS azide.<sup>8</sup>

The data associated with this extended SAR are summarized in [Table 2](#). As illustrated, the position of the carboxylic acid was critical with essentially all activity being lost when this group was moved to the 3-position (**7g**). Further supporting the importance of the positioning of the carboxylic acid is the loss in potency resulting in one-carbon homologation (**7h**). Maintaining an acidic pH was demonstrated necessary when noting the reduced activity resulting from replacing the carboxylic acid with a dimethylamino group (**7i**). Like the ester (**7e**, [Table 1](#)), the methyl amide (**7j**) failed to demonstrate an advantage. This was also noted with the tetra-

**Keywords:** Calmodulin; Kinase; Inhibitors; Pyrimidines.

\* Corresponding author. Tel.: +1 650 704 3051; e-mail: [del345@gmail.com](mailto:del345@gmail.com)



**Scheme 1.** Reagents and conditions: (a)  $\text{Pd}[\text{P}(\text{Ph})_3]_4$ ,  $\text{Na}_2\text{CO}_3$ ,  $\text{CH}_3\text{CN}$ ,  $90^\circ\text{C}$ , 4 h, 50–60%; (b)  $\text{Pd}(\text{OAc})_2$ ,  $\text{Cs}_2\text{CO}_3$ , BINAP, dioxane,  $90^\circ\text{C}$ , 20 h, 65–80%; (c)  $\text{H}_2$ , 10%Pd/C, EtOH, 40 psi, 24–48 h, 95%.

**Table 1.** SAR of initial pyrimidine-based leads

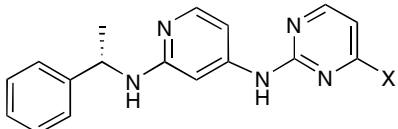
Compound	X	IC <sub>50</sub> (μM)
7a		1.28 ( <i>n</i> = 1)
7b		3.14 ( <i>n</i> = 1)
7c		0.92 ( <i>n</i> = 1)
7d		2.87 ( <i>n</i> = 1)
7e		1.69 ± 0.47 ( <i>n</i> = 3)
7f		0.21 ± 0.01 ( <i>n</i> = 2)

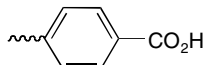
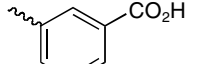
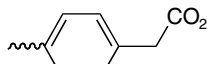
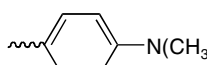
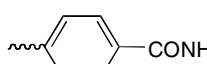
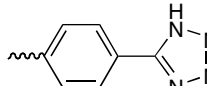
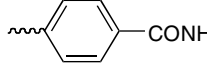
zole (7k) introduced as a carboxylic acid isostere. In fact, the only additional analog demonstrating sub-micromolar activity was the hydroxamic acid (7l). All results can be explained by recognizing that non-acidic groups or acidic groups in sub-optimal positions are not able to optimally interact with Lys22 at the entrance to the ATP site as predicted by our homology model.

With compound 7f remaining as our lead analog, our next exercise was to determine the minimum active

structure of this series. This was accomplished by systematically carving away the structural components of 7f and testing the activity of the resulting analogs. The compounds of this new SAR were prepared according to Scheme 2. As illustrated, dichloropyrimidine was coupled with a boronic acid under Suzuki conditions. Subsequent Buchwald coupling of anilines with the resulting chloropyrimidine followed by the base hydrolysis of the methyl esters gave target compounds 11. For compound 11a, the aniline utilized was prepared by coupling *p*-methoxybenzylamine with compound 4 followed by the reduction of the nitro group to an amine (Scheme 1). Subsequent cleavage of the *p*-methoxybenzyl group was achieved by treating the ester analog with trifluoroacetic acid. Compounds 11b, 11c, and 11d were prepared using commercially available anilines and aminopyridines.

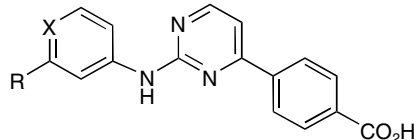
As shown in Table 3, elimination of the methylbenzyl group resulted in a 3-fold increase in activity against CaMKIIδ. However, when the resulting amine was removed, the activity trended lower. The true breakthrough came when the pyridyl group was replaced with a phenyl. This modification resulted in a 3-fold increase in activity over our previous lead 7f. Furthermore, by utilizing our homology model, 11c was predicted to be capable of entering the ATP site and making a dual hydrogen bond interaction between the hinge region and the aminopyrimidine unit. Additionally, modeling also suggested that the carboxylic acid was now forming a new salt bridge with Lys43 within the ATP site while the phenyl group was filling a hydrophobic pocket. Additional enhancement of activity was noted by introducing a chloro group to the *meta* position of the phenyl ring in order to maximize the occupation of the hydrophobic pocket. This resulted in an additional benefit to activity.

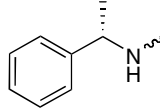
**Table 2.** SAR surrounding the carboxylic acid of **7f**


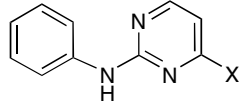
Compound	X	IC <sub>50</sub> (μM)
<b>7f</b>		0.21 ± 0.01 (n = 2)
<b>7g</b>		12.99 (n = 1)
<b>7h</b>		3.42 ± 0.33 (n = 2)
<b>7i</b>		2.22 (n = 1)
<b>7j</b>		0.72 ± 0.39 (n = 2)
<b>7k</b>		2.26 ± 0.21 (n = 2)
<b>7l</b>		0.17 (n = 1)

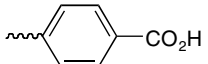
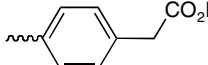
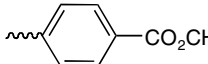
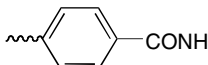
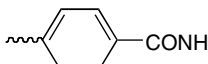
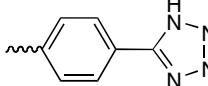
Having identified **11c** as the critical active structure, the SAR applied to the carboxylic acid region of **7f** was applied to our new lead. The compounds of this SAR were prepared using chemistry illustrated or described in this report and the data are summarized in Table 4. As illustrated and supported by the data in Table 2, the presence and positioning of an acidic group was essential for activity. In fact, where a carboxylic acid and a hydroxamic acid were essentially interchangeable in Table 2 SAR, Table 4 shows this modification to result in a 5-fold loss in activity when applied to **11c**.

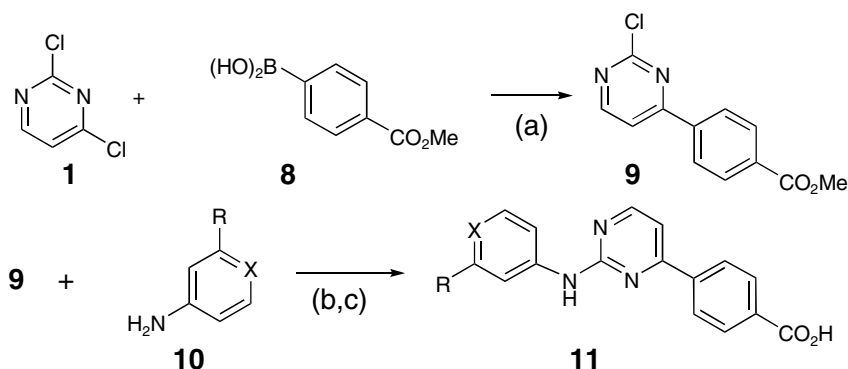
Advancing from direct binding assays, CaMKIIδ-mediated phosphorylation of vimentin was studied in whole cell systems and modulation of this process was mea-

**Table 3.** SAR resulting from structural minimization of **7f**


Compound	R	X	IC <sub>50</sub> (μM)
<b>7f</b>		N	0.21 ± 0.01 (n = 2)
<b>11a</b>	H <sub>2</sub> N	N	0.066 (n = 1)
<b>11b</b>	H	N	0.39 ± 0.10 (n = 2)
<b>11c</b>	H	CH	0.064 ± 0.031 (n = 2)
<b>11d</b>	Cl	CH	0.042 ± 0.007 (n = 2)

**Table 4.** SAR surrounding the carboxylic acid of **11c**


Compound	X	Enzyme IC <sub>50</sub> (μM)	Cell-based %I at 5 μM
<b>11c</b>		0.064±0.031 (n = 2)	0
<b>11e</b>		>20 (n = 1)	
<b>11f</b>		>20 (n = 1)	0
<b>11g</b>		>20 (n = 1)	
<b>11h</b>		0.29 (n = 1)	90
<b>11i</b>		0.77 (n = 1)	0



**Scheme 2.** Reagents and conditions: (a) Pd[P(Ph)<sub>3</sub>]<sub>4</sub>, Na<sub>2</sub>CO<sub>3</sub>, CH<sub>3</sub>CN, 90 °C, 4 h, 50–60%; (b) Pd(OAc)<sub>2</sub>, Cs<sub>2</sub>CO<sub>3</sub>, BINAP, dioxane, 90 °C, 20 h, 75–85%; (c) NaOH, MeOH, H<sub>2</sub>O, 95%.

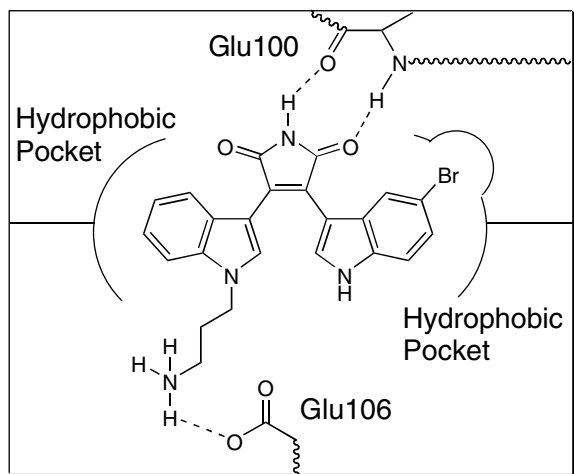


Figure 1. Amine-based maleimides interact with Glu106.

sured as a function of inhibitor concentration.<sup>9</sup> As shown in Table 4, there was initially no significant cellular activity noted for our inhibitors. Recognizing the value of tetrazoles and hydroxamic acids as carboxylic acid isosteres, these groups were studied for their potential to improve cell penetrance. As shown, only the hydroxamic acid exhibited interesting activity. Therefore, with a narrow SAR for aryl functionality and the poor cellular activity of acid-based inhibitors, we sought new alternatives.

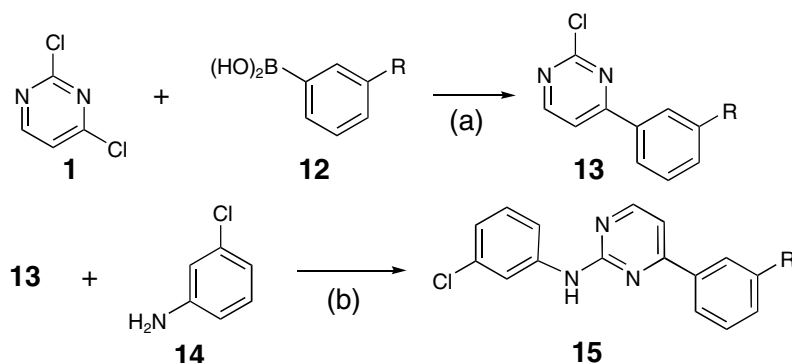
Turning to work presented in previous publications,<sup>1–3</sup> we recognized that our homology model indicated that the amine tether of our maleimide inhibitors interacted with Glu106 (Fig. 1). Furthermore, our model placed Glu106 in close proximity to Lys43. Using this information, coupled with computational docking studies in the homology model ATP site as well as solvation energy calculations,<sup>10</sup> compounds were designed with acidic groups at the aryl 4-position replaced with basic groups at the aryl 3-position. Preparation of these analogs, illustrated in Scheme 3 involved Suzuki couplings of boronic acids with dichloropyrimidine. Subsequent Buchwald coupling with 3-chloroaniline gave the target compounds 15. For analogs 15a, 15b, and 15e, the sequence was executed using boronic acids with Boc-protected amines. Formation and cleavage of the

Table 5. SAR surrounding amine-substituted aryl groups

Compound X		Enzyme IC <sub>50</sub> (μM)	Cell-based IC <sub>50</sub> (μM)
11d		0.042 ± 0.007 (n = 2)	0% I at 5 μM
15a		0.66 ± 0.04 (n = 2)	
15b		0.009 (n = 1)	0.32 (n = 1)
15c		0.24 ± 0.05 (n = 2)	
15d		0.93 ± 0.04 (n = 2)	
15e		0.012 (n = 1)	0.11 (n = 1)

Boc-protecting group was achieved under standard conditions. Furthermore, the boronic acid required for 15e was prepared by first treating 3-bromoaniline with Boc-2-bromoethylamine followed by conversion of the bromide to the required pinacolboronic ester.

Assay results of the amine-based compounds are shown in Table 5 and compared to the parent carboxylic acid analog, 11d. As illustrated, replacing the 4-carboxylic acid with a 3-amino group resulted in a significant drop in potency. This confirmed the modeling prediction that a simple aniline could not reach Glu106. However, when the amine was replaced with a piperazine, a significant



Scheme 3. Reagents and conditions: (a) Pd[P(Ph)<sub>3</sub>]<sub>4</sub>, Na<sub>2</sub>CO<sub>3</sub>, CH<sub>3</sub>CN, 90 °C, 4 h, 50–60%; (b) Pd(OAc)<sub>2</sub>, Cs<sub>2</sub>CO<sub>3</sub>, BINAP, dioxane, 90 °C, 20 h, 75–85%.

improvement in activity was noted. In fact, compound **15b** demonstrated that we could overcome cell penetration issues with sub-micromolar activity in our cell-based assay. Furthermore, we validated the importance of the extended basic group using morpholine or piperidine as piperazine variants. In both cases, enzyme activity was compromised. Finally, an unexpected benefit resulted from relaxing the positioning of the extended amine by replacing the piperazine with ethylene diamine. While this compound showed no improvement in enzyme activity, a 3-fold increase in cellular activity was noted.

In summary, novel pyrimidine-based inhibitors of CaMKII $\delta$  were prepared. Homology model predictions were used to advance the SAR from micromolar inhibitors to low nanomolar inhibitors. Activity in cell-based assays was improved by introducing basic groups at the phenyl 3-position and generating a predicted salt bridge with Glu106. Our most potent inhibitor possessed a flexible tether to the amine and exhibited an IC<sub>50</sub> of 12 nM against the isolated enzyme.

#### References and notes

1. Levy, D. E.; Wang, D.-X.; Lu, Q.; Chen, Z.; Perumattam, J.; Xu, Y.-J.; Licican, A.; Higaki, J.; Dong, H.; Laney, M.; Mavunkel, B.; Dugar, S. *Bioorg. Med. Chem. Lett.* **2008**, *18*, 2390.
2. Levy, D. E.; Wang, D.-X.; Lu, Q.; Chen, Z.; Perumattam, J.; Xu, Y.-J.; Higaki, J.; Dong, H.; Licican, A.; Laney, M.; Mavunkel, B.; Dugar, S. *Bioorg. Med. Chem. Lett.* **2008**, *18*, 2395.
3. Lu, Q.; Chen, Z.; Perumattam, J.; Wang, D.-X.; Liang, W.; Xu, Y.-J.; Do, S.; Bonaga, L.; Higaki, J.; Dong, H.; Licican, A.; Sideris, S.; Laney, M.; Dugar, S.; Mavunkel, B.; Levy, D. E. *Bioorg. Med. Chem. Lett.* **2008**, *18*, 2399.
4. Zapf, A. In *Transition Metals for Organic Synthesis: Building Blocks and Fine Chemicals*, 2nd ed.; Beller, M., Bolm, C., Eds.; Wiley-VCH: Weinheim, 2004; p 1344.
5. Wolfe, J. P.; Buchwald, S. L. *J. Org. Chem.* **2000**, *65*, 1144.
6. Assays were performed with inhibitor or suitable control solvent added 10  $\mu$ l per well in a 96-well microtiter plate (Corning, NY). CaMKII $\delta$  was diluted in enzyme buffer (50 mM PIPES, pH 7, 0.2 mg/ml BSA, 1 mM DTT) and added 10  $\mu$ l per well. Reactions were initiated with 30  $\mu$ l reaction buffer (62.5 mM PIPES, pH 7, 0.25 mg/ml BSA, 33.3 mM MgCl<sub>2</sub>, 83  $\mu$ M ATP, 0.4 mM CaCl<sub>2</sub>, 8.3  $\mu$ g/ml calmodulin, 25  $\mu$ M [His 5] Autocamtide-2, 120 nM [g-33P]ATP) and incubated at RT for 3 min. Reactions were terminated by transferring 25  $\mu$ l to a UNIFILTER 96-well P81 microplate (Whatman, UK), pre-wet with 15  $\mu$ l 1% phosphoric acid. After 10 min, the plate was washed three times with 1% phosphoric acid and one time with 95% ethanol on a BiomekFX (Beckman-Coulter, CA) equipped with a vacuum manifold. Plates were dried for approximately 60 min, scintillant was added to the wells, and the plates were read on a TopCount NXT Microplate Scintillation and Luminescence Counter (Perkin-Elmer, MA).
7. An homology model of autoinhibited CaMKII $\delta$  was built based on the crystal structure 1A06 of autoinhibited rat CaMKI. Because rat CaMKI shows high sequence homology with CaMKII $\delta$ , this model was used to study inhibitors that were not ATP competitive. Due to the lack of availability of a crystal structure of activated CaMKII $\delta$ , homology models were built based on crystal structures 1CDK, 1PHK, and 1KOB. From these homology models, we selected the one best explained the SAR. The accuracy of this model was validated using point mutation studies.
8. Amantini, D.; Beleggia, R.; Fringuelli, F.; Pizzo, F.; Vaccaro, L. *J. Org. Chem.* **2004**, *69*, 2896.
9. HL-2 cells were pre-incubated with increasing concentrations of an inhibitor for 1 h at 37 °C. CaMKII was activated by cell treatment with 1  $\mu$ M ionomycin for 15 min at 37 °C. Cells were then lysed in ice-cold M-PER cell lysis buffer (Pierce) and frozen at –80 °C. Inhibitor IC<sub>50</sub> values were determined by an ELISA assay of cell lysate measuring intracellular vimentin phosphorylated at Ser82 (Delling, Catalano, Wang, Higgins, unpublished).
10. Solvation energy calculations were generated using ZAP (Openeye Scientific Software).